



OPEN

Assessment of transthyretin instability in patients with wild-type transthyretin amyloid cardiomyopathy

Takuya Iino^{1,2}, Manabu Nagao^{3✉}, Hidekazu Tanaka¹, Sachiko Yoshikawa¹, Junko Asakura¹, Makoto Nishimori⁴, Masakazu Shinohara^{4,5}, Amane Harada², Shunsuke Watanabe⁶, Tatsuro Ishida^{1,7}, Ken-ichi Hirata^{1,3} & Ryuji Toh³

The pathophysiology of variant transthyretin (TTR) amyloidosis (ATTRv) is associated with destabilizing mutations in the TTR tetramer. However, why TTR with a wild-type genetic sequence misfolds and aggregates in wild-type transthyretin amyloidosis (ATTRwt) is unknown. Here, we evaluate kinetic TTR stability with a newly developed ELISA system in combination with urea-induced protein denaturation. Compared with that in control patients, endogenous TTR in patients with wild-type transthyretin amyloid cardiomyopathy (ATTRwt-CM) exhibited thermodynamic instability, indicating that circulating TTR instability may be associated with the pathogenesis of ATTRwt as well as ATTRv. Our findings provide new insight into the underlying mechanisms of ATTRwt.

Keywords Transthyretin, Wild-type transthyretin amyloid cardiomyopathy, Heart failure, Heart failure with preserved ejection fraction, Aging

Abbreviations

TTR	Transthyretin
ATTR	Transthyretin amyloidosis
ATTRv	Variant transthyretin amyloidosis
ATTRwt	Wild-type transthyretin amyloidosis
ATTR-CM	Transthyretin amyloid cardiomyopathy
ATTRv-CM	Variant transthyretin amyloid cardiomyopathy
ATTRwt-CM	Wild-type transthyretin amyloid cardiomyopathy
ELISA	Enzyme-linked immunosorbent assay
HF	Heart failure
HFpEF	Heart failure with preserved ejection fraction

Transthyretin (TTR) amyloidosis (ATTR) is a systemic disease caused by deposition of TTR-derived amyloid in various organs represented by the peripheral nervous system and heart¹. TTR is a 127-amino acid, 55-kDa homotetrameric protein that is synthesized mainly in the liver and functions as a transporter of thyroxine and retinol-binding protein in the bloodstream². The TTR tetramer is known to dissociate into an aggregation-prone monomer that forms amorphous aggregates and subsequent amyloid fibrils, leading to tissue dysfunction and clinical phenotypes of ATTR^{3–5}. ATTR is classified as wild-type transthyretin amyloidosis (ATTRwt, nonhereditary form) or variant transthyretin amyloidosis (ATTRv, hereditary form) according to the presence or absence of TTR genetic mutations. Previous studies have reported that ATTRv pathophysiology is associated

¹Division of Cardiovascular Medicine, Kobe University Graduate School of Medicine, Kobe, Japan. ²Central Research Laboratories, Sysmex Corporation, Kobe, Japan. ³Division of Evidence-Based Laboratory Medicine, Kobe University Graduate School of Medicine, 7-5-1 Kusunoki-Cho, Chuo-Ku, Kobe 650-0017, Japan. ⁴Division of Molecular Epidemiology, Kobe University Graduate School of Medicine, Kobe, Japan. ⁵The Integrated Center for Mass Spectrometry, Kobe University Graduate School of Medicine, Kobe, Japan. ⁶Bio-Diagnostic Reagent Technology Center, Sysmex Corporation, Kobe, Japan. ⁷Division of Nursing Practice, Kobe University Graduate School of Health Sciences, Kobe, Japan. ✉email: mnagao@med.kobe-u.ac.jp

with destabilizing mutations in the TTR tetramer, but the mechanisms involved in the development of ATTRwt remain unknown^{6,7}.

Over the past decade, transthyretin amyloid cardiomyopathy (ATTR-CM) has been recognized as a significant cause of HF and has been increasingly diagnosed due to advances in noninvasive imaging modalities, including cardiac bone scintigraphy with diphosphonate or pyrophosphate tracers. Although ATTR-CM is thought to be a rare disorder, an improved imaging modality and newly emerging therapies, such as TTR stabilizers⁸ or small interfering RNA drugs^{9,10}, have facilitated recognition of the disease, as did epidemiological studies, which indicate that there are likely more undiagnosed ATTR-CM patients¹¹. Indeed, 16% of patients with severe aortic stenosis who underwent transcatheter aortic valve replacement were positive by technetium-99 m pyrophosphate (^{99m}Tc-PYP) scintigraphy, an established diagnostic imaging method for ATTR-CM¹². With a particular focus on wild-type ATTR-CM (ATTRwt-CM), approximately 13% of patients with heart failure with preserved ejection fraction (HFpEF) with left ventricular hypertrophy (LVH) are diagnosed with ATTRwt-CM¹³. In another cohort, approximately 20% of HF patients with LVH had ATTRwt-CM¹⁴. As wild-type ATTR was previously called senile systemic amyloidosis, the average age of patients with ATTRwt-CM was greater than that of patients with variant transthyretin amyloid cardiomyopathy (ATTRv-CM), suggesting the strong association of ATTRwt-CM with aging^{11,15}. In addition, a recent study reported that approximately 80% of patients older than 70 years of age with ATTR-CM had ATTRwt-CM¹⁵. Taken together, these findings suggest that ATTRwt-CM may be underestimated as a cause of HF in elderly individuals.

Importantly, stabilizing the TTR tetramer with the TTR stabilizer tafamidis improves the prognosis of ATTRwt-CM patient⁸, suggesting that instability of the TTR tetramer is associated with the pathophysiology of not only ATTRv but also ATTRwt without destabilizing mutations. Nevertheless, there is no direct evidence proving TTR instability in ATTRwt. In this study, we sought to demonstrate TTR instability in patients with ATTRwt-CM by using a newly developed enzyme-linked immunosorbent assay (ELISA) system with urea unfolding. The findings may contribute to the development of new diagnostic procedures, leading to early detection of elderly HF patients based on ATTRwt-CM.

Results

First, we purchased recombinant wild-type TTR and monomeric variant TTR (F87M/L110M) and analyzed the size of each protein using gel filtration chromatography. The results confirmed that the calculated molecular weight of wild-type TTR was approximately four times greater than that of F87M/L110M, suggesting that recombinant wild-type TTR forms tetramers (Fig. 2A,B). Next, using the same anti-TTR antibody for both capture and detection, we developed a new ELISA system that specifically reacts with the TTR tetramer (Fig. 1) and subsequently identified the specificity of the tetrameric recombinant wild-type TTR and TTR purified from human plasma; however, the ELISA did not detect the monomeric variant TTR (Fig. 2C, Supplementary Table 1). The comparable reactivity of tetrameric recombinant wild-type TTR and TTR purified from human plasma suggested the formation of a tetrameric structure in TTR within human blood samples. The assay performance of the ELISA was validated through calibration curve analysis, dilution linearity of serum, and intra- and inter-assay precision (Supplementary Tables 2, 3, 4).

Next, we incubated recombinant TTRs, including wild-type TTR and 3 types of variants (V30M, T119M, and V122I), in the presence of several concentrations of urea for 48 h at 25 °C. After incubation, each sample was diluted 6180 times to mitigate the inhibitory effects of urea on ELISA and to bring the TTR concentration within the quantification range of the ELISA. We determined the residual TTR tetramer percentage via a new ELISA. The residual TTR tetramer ratio of all the TTRs decreased in a urea concentration-dependent manner (Fig. 3A). The dissociation tendency revealed that TTR with the T119M mutation, a stable variant, exhibited kinetic stability comparable with that of wild-type TTR; conversely, TTR with the V30M and V122I mutations, unstable variants, was less stable than was the wild-type TTR (Fig. 3A). The significant difference between T119M and V30M and V122I was most pronounced at 7.2 mol/L urea (Supplementary Figure S1, Fig. 3B). Therefore, we adopted 7.2 mol/L urea as the pretreatment condition for evaluating TTR stability. To determine whether this new assay reflects TTR stability in serum, we incubated human serum with or without the TTR stabilizer tafamidis under urea conditions. As expected, compared with the control vehicle, tafamidis enhanced the residual TTR tetramer concentration in the serum (Fig. 4). These data indicate that the developed assay can evaluate TTR stability *in vitro*.

Finally, we sought to measure endogenous TTR stability in ATTRwt-CM patients. As a control, we enrolled age- and sex-matched patients with arrhythmia and excluded patients with LVH and CTS to eliminate the possibility that the control group included undiagnosed ATTRwt patients. Therefore, the number of patients with atrial fibrillation was significantly greater in the control group than in the ATTRwt-CM group. The detailed patient characteristics are shown in Table 1. With respect to quantification of TTR, we confirmed the strong correlation between the immunoturbidimetry method commonly used in clinical assays and the developed ELISA (Supplementary Figure S2). However, the serum TTR concentration did not significantly differ between the ATTRwt-CM group and the control group (Fig. 5A). On the other hand, the residual TTR tetramer ratio was significantly lower in the ATTRwt-CM group than in the control group {median (IQR), control; 65.8 (63.05–69.8), ATTRwt-CM; 62.5 (57.58–66.5), *p* value = 0.0289} (Fig. 5B). These results indicate that measuring the residual TTR tetramer ratio after urea denaturation is more effective at determining TTR stability than merely measuring the serum concentration of TTR itself. Although the sample size was too small to assess the difference statistically, the percentages of ATTRv-CM and ATTRwt-CM patients taking tafamidis tended to be lower and greater, respectively, than those in the control group (Fig. 5B).

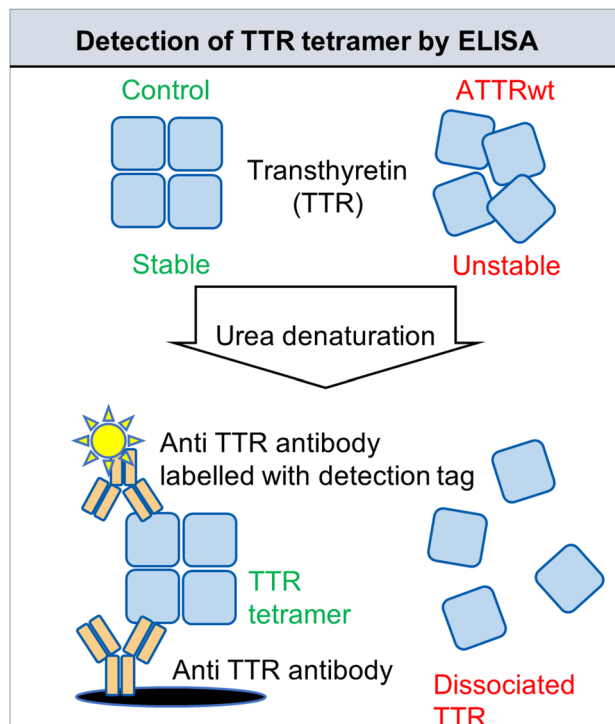


Fig. 1. Workflow for assessment of TTR stability under urea conditions. TTR-containing samples were diluted tenfold with PBS containing 0–8 mol/L urea, resulting in a final concentration of 0–7.2 mol/L urea, and incubated at 25 °C for 48 h. After incubation, the samples were diluted 6180 times with PBS containing 1% BSA and applied to ELISA plate wells immediately after dilution. Tetrameric TTR levels in the samples were quantified via ELISA in duplicate. TTR stability under urea conditions was evaluated as the residual TTR tetramer percentage. ATTRwt, wild-type transthyretin amyloidosis; TTR, transthyretin; ELISA, enzyme-linked immunosorbent assay.

Discussion

Due to the lack of systematic evidence, the overall population of ATTRwt patients has not been fully characterized. Recent studies, however, have reported that the incidence of ATTRwt-CM is high among patients with HFpEF, patients with CTS, and elderly patients with aortic stenosis^{16,17}. Given the high prevalence and the fact that amyloid fibril deposits are mainly located in heart tissue¹⁸, cost-effective and noninvasive laboratory tests for ATTRwt-CM are becoming increasingly important. In the present study, we developed an ELISA system that reacts with only the TTR tetramer, which enabled evaluating the stability of the TTR tetramer in combination with a urea denaturation assay. By applying this method to the serum of ATTRwt-CM patients, we confirmed the instability of endogenous TTR in these patients, suggesting that TTR instability is partly associated with pathogenesis, even in ATTRwt-CM.

There are more than 130 pathogenic TTR variants involved in ATTRv¹¹, and several mutations increase susceptibility of TTR to dissociation due to kinetic instabilities⁴; however, why TTR with a wild-type genetic sequence misfolds and aggregates in ATTRwt is unclear⁵. In this regard, age is the major risk factor for ATTRwt. The standard age of onset for ATTRwt-CM is in the seventh or eighth decade of life^{15,19}. Zhao et al. hypothesized that age-associated TTR oxidation is a causal factor of ATTRwt and showed that recombinant wild-type TTR with oxidative modifications is more likely to be thermodynamically unstable and to form aggregates than nonoxidative controls²⁰.

Unlike previous studies using recombinant TTR, we assessed the residual percentage of endogenous TTR tetramers with a specific antibody after urea-mediated protein denaturation. Our data indicates that a portion of the circulating TTR is unstable in ATTRwt-CM patients before local deposition. In support of this notion, circulating aggregated TTR was hypothesized to be the pathogenic driver of ATTR and was successfully detected by ELISA with specific antibodies against aggregated TTR in blood samples from patients with both ATTRv and ATTRwt^{21,22}. However, where (in the circulation or at the local site of deposition) and how the TTR tetramer becomes unstable and dissociates are not completely understood. In addition, these antibody-based methods have still not been established as laboratory tests for ATTR.

The most prominent difference between our study and previous studies that sought to detect circulating TTR monomers or aggregates is that our assay focused on the residual percentage of TTR tetramers in patient serum. The evidence that this assay correctly reflects TTR stability is as follows. (1) Recombinant TTR with a stable mutation (T119M) presented the highest residual percentage of the TTR tetramer. (2) Addition of tafamidis to patient serum inhibited urea-induced TTR dissociation *in vitro*. (3) ATTRwt-CM patients given tafamidis showed a trend toward increased TTR stability. In contrast, by using another method called the subunit exchange

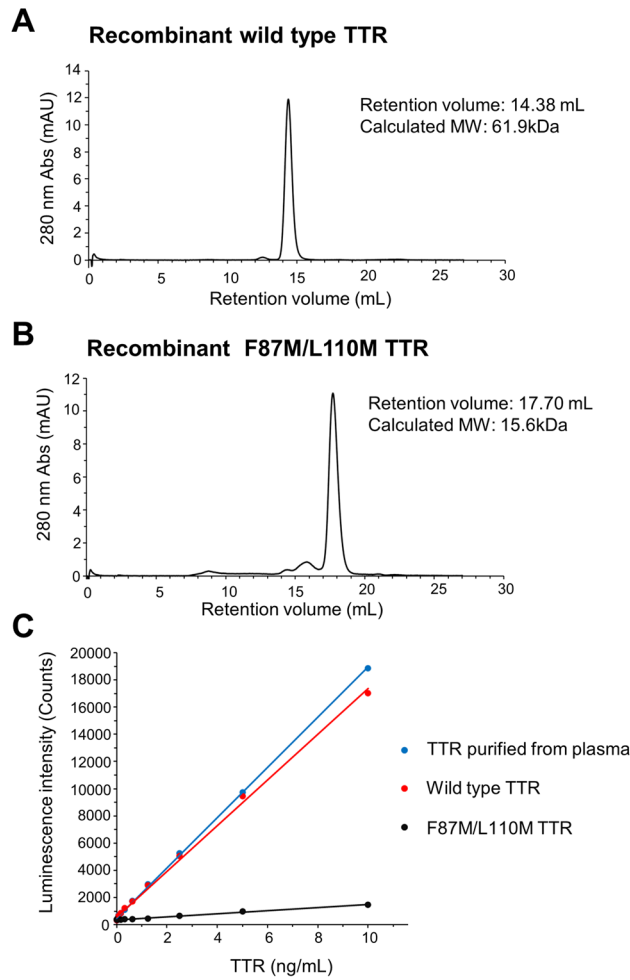


Fig. 2. Development of an ELISA for specific reactions to the TTR tetramer. Chromatogram of recombinant wild-type TTR (A) and recombinant F87M/L110M TTR (B) obtained by gel filtration chromatography. ELISA data for recombinant wild-type TTR, recombinant F87M/L110M TTR, and TTR purified from human plasma (C). Standard curves were generated using a linear calibration model. TTR, transthyretin; MW, molecular weight; Abs, absorbance.

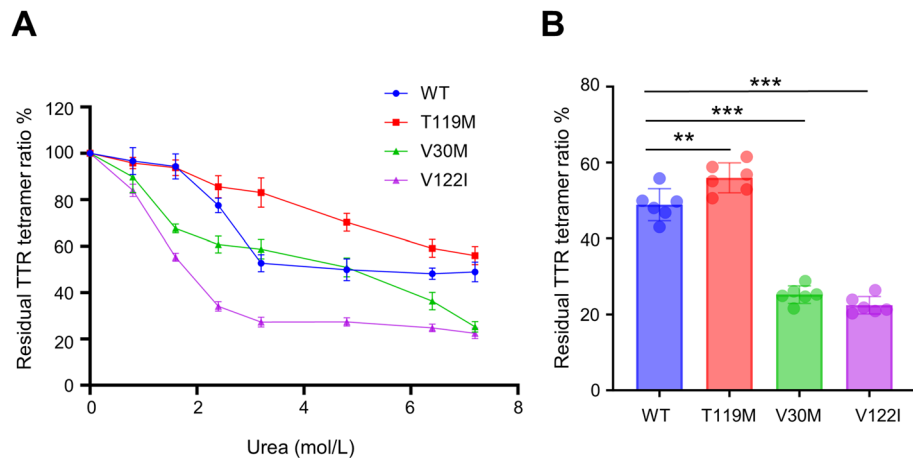


Fig. 3. Assessment of TTR variant stability. The residual TTR tetramer percentage (%) after urea-induced denaturation of recombinant wild-type TTR, recombinant T119M TTR, recombinant V30M TTR, and recombinant V122I TTR (A). Comparison of the residual TTR tetramer formation ratio of TTRs after 7.2 mol/L urea treatment (B). Values are expressed as means \pm SDs ($n = 6$). ** $p < 0.01$, *** $p < 0.001$. Data were analyzed by one-way ANOVA with Dunnett’s multiple comparisons test. TTR, transthyretin; WT, wild-type.

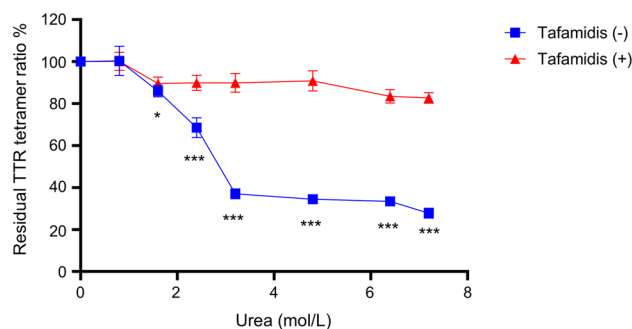


Fig. 4. Effects of tafamidis on TTR stability in serum. The residual TTR tetramer ratio after urea-induced denaturation of TTR in serum and TTR in serum preincubated with 500 $\mu\text{mol/L}$ tafamidis at room temperature for 30 min. Values are expressed as the means \pm SDs ($n = 6$). * $p < 0.05$, *** $p < 0.001$ compared to the control vehicle. Data were analyzed by the unpaired Student's t test. TTR, transthyretin.

	Control	ATTRwt-CM	<i>p</i> value
Number	25	18	
Age, years, mean \pm SD	73.1 \pm 3.9	75.5 \pm 6.2	0.142
Female, n (%)	4 (16.0)	3 (16.6)	0.953
BMI, kg/m ² , mean \pm SD	23.2 \pm 3.9	22.8 \pm 3.5	0.752
Comorbidities, n (%)			
Atrial fibrillation, n (%)	22 (88.0)	6 (33.3)	< 0.001
Coronary artery disease, n (%)	2 (8.0)	0 (0.0)	0.219
History of heart failure, n (%)	6 (24.0)	16 (88.8)	< 0.001
Carpal tunnel syndrome, n (%)	0 (0)	8 (44.4)	< 0.001
Hypertension, n (%)	11 (44.0)	8 (44.4)	0.997
Diabetes mellitus, n (%)	6 (24.0)	3 (16.6)	0.560
Echocardiographic parameters			
LVDD, mm	47.2 \pm 5.9	42.3 \pm 8.1	0.033
LVDS, mm	32.7 \pm 7.2	34.2 \pm 8.5	0.528
LVEF, %	60.5 [55.0–64.4]	46.3 [37.4–53.7]	< 0.001
IVST, mm	9.1 \pm 1.3	15.1 \pm 3.6	< 0.001
PWT, mm	9.3 [7.8–10.9]	14.9 [12.8–19.8]	< 0.001
Laboratory data			
Creatinine, mg/dL	0.85 \pm 0.13	1.23 \pm 0.53	0.001
eGFR, mL/min/1.73m ²	61.6 [56.7–70.1]	50.5 [31.2–67.4]	0.012
BNP, pg/mL	52.6 [27.3–97.2]	218.8 [136.0–380.7]	< 0.001
HbA1c, %	5.8 [5.6–6.1]	5.9 [5.6–6.4]	0.651
Medications			
Tafamidis	0	0	–
Loop diuretic, %	20.0	61.1	0.006
MRA, %	20.0	50.0	0.038
B-blocker, %	44.0	66.6	0.142
ACEI/ARB, %	28.0	27.7	0.987
ARNI, %	8.0	16.6	0.382
SGLT-2i, %	16.0	33.3	0.184

Table 1. Baseline characteristics. Continuous variables are shown as the mean \pm standard deviation for normally distributed data or as medians with interquartile ranges for nonnormally distributed data. *SD* standard deviation, *BMI* body mass index, *LVDD* left ventricular diameter at end diastole, *LVDS* left ventricular diameter at end systole, *LVEF* left ventricular ejection fraction, *IVST* interventricular septum thickness, *PWT* posterior wall thickness, *eGFR* estimated glomerular filtration rate, *BNP* brain natriuretic peptide, *HbA1c* hemoglobin A1c, *MRA* mineral corticoid receptor antagonist, *ACEI* angiotensin-converting enzyme inhibitor, *ARB* angiotensin II receptor blocker, *ARNI* angiotensin receptor neprilysin inhibitor, *SGLT-2i* sodium glucose cotransporter-2 inhibitor.

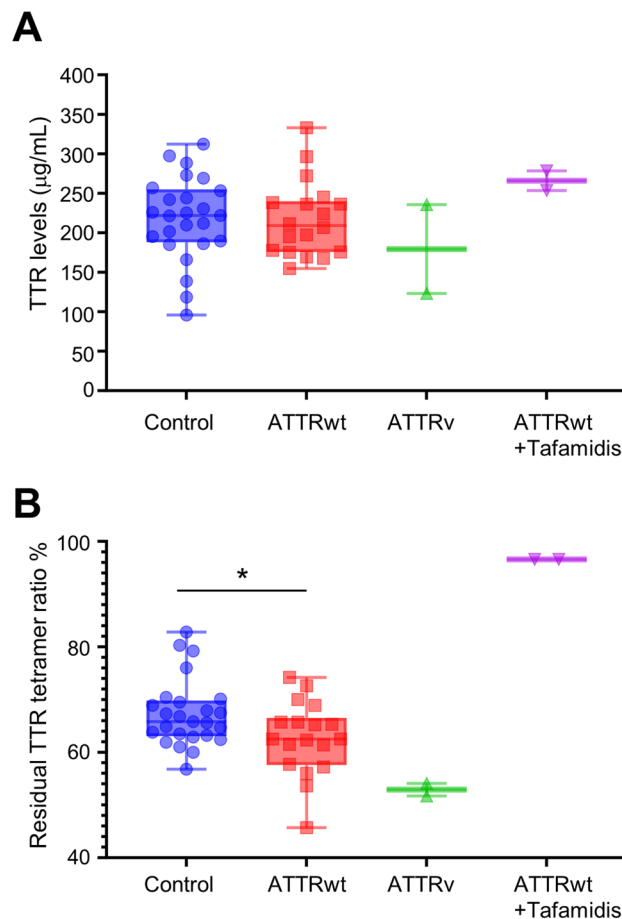


Fig. 5. Assessment of TTR stability in ATTRwt-CM patients. TTR in serum was determined by immunoturbidimetry (**A**). The residual TTR tetramer percentage (%) after urea-induced denaturation of TTR in serum (**B**). Values are presented with medians {interquartile range (IQR)}. * $p < 0.05$. Data were analyzed by the unpaired Student's *t* test. Control ($n = 25$), ATTRwt ($n = 18$, patients not treated with tafamidis), ATTRv ($n = 2$, patients not treated with tafamidis), ATTRwt + Tafamidis ($n = 2$, patients treated with tafamidis). ATTRwt, wild-type transthyretin amyloid cardiomyopathy; ATTRv, variant transthyretin amyloid cardiomyopathy; TTR, transthyretin; NS, not significant.

assay, Rappley et al. demonstrated that the stability of endogenous TTR in the plasma of ATTRwt patients did not exhibit a significant difference compared to that of the age-matched controls²³. Although this discrepancy may be partly attributed to differences in methodology and study subjects, we need to uncover the underlying cause of the variations in results.

This study has several limitations. First, the study was limited by its single-center nature and small sample size. Larger samples are required to validate our findings and to reduce selection bias in the study population. Second, we were not able to determine the biological mechanisms by which the TTR tetramer in ATTRwt-CM patients becomes unstable and dissociates into monomers. Third, many hours are required to assess TTR stability if the assay is considered a screening test as a possible future direction. Lastly, the ELISA developed in this study employs the same antibody for both capture and detection, potentially detecting not only tetramers but also dimers and trimers. However, the effects of these oligomeric species were not assessed in this study. Further elucidation and improvement of the assay are needed to address these issues.

Conclusions

To our knowledge, this is the first study to directly evaluate TTR stability by using blood samples from ATTRwt-CM patients and a new ELISA system. In the next step, using the new assay, we need to validate the instability of circulating TTR in another dataset of ATTRwt patients and demonstrate that endogenous TTR instability may be associated with the pathophysiology of both ATTRwt and ATTRv.

Methods

Preparation of blood samples and ethical considerations

The Kobe Cardiovascular Marker Investigation registry, a single-center registry of patients referred to Kobe University Hospital with CVD, was used to identify blood-based biomarkers that are effective at predicting

CVD incidence. The study protocol was in accordance with the ethical guidelines of the 1975 Declaration of Helsinki. The study was approved by the Ethics Review Committee of Kobe University (Japan). Written informed consent was obtained from all patients before enrollment in the study.

From January 2021 to December 2022, blood samples were obtained at Kobe University Hospital in the morning after overnight fasting. The serum was immediately separated by centrifugation and frozen at $-80\text{ }^{\circ}\text{C}$ until analysis. All serum samples were thawed at room temperature and used for the assays. No more than 2 cycles of freeze–thaw were applied, as described in the previous report²⁴. Twenty-two consecutive ATTR-CM patients (ATTRwt;20, ATTRv;2) were enrolled. To diagnose ATTRwt-CM, all patients underwent endomyocardial or extracardiac biopsy with evidence of Grade 2–3 imaging score by $^{99\text{m}}\text{Tc}$ -pyrophosphate (PYP) scintigraphy, followed by amyloid typing and genotyping to confirm TTR deposition and detect any variants of the TTR gene, respectively. As a control, blood samples were collected from 25 age- and sex-matched patients who underwent catheter ablation for cardiac arrhythmias and did not exhibit left ventricular hypertrophy (LVH) (interventricular septum thickness; IVST $< 12\text{ mm}$) according to echocardiography or carpal tunnel syndrome (CTS). Both of these features are clinically typical features of ATTR-CM²⁵.

Proteins and antibodies

The proteins used in this study were as follows: recombinant wild-type TTR (AlexoTech, #T-500-10), recombinant V30M TTR (AlexoTech, #T-505-10), recombinant V122I TTR (AlexoTech, #T-507-10), recombinant T119M TTR (AlexoTech, #T-515-10), recombinant F87M/L110M TTR (AlexoTech, #T-509-10), and TTR purified from human plasma (Athens Research & Technology, #16-161,801). The antibody used to detect the TTR tetramer was an anti-transferrin polyclonal antibody (Agilent, #A0002).

ELISA

One hundred microliters of $2\text{ }\mu\text{g/mL}$ of the anti-transferrin polyclonal antibody in PBS was added to the wells of a 96-well black-bottom microplate (Sumitomo Bakelite, #MS-8596 K), and the plate was incubated overnight. After the wells were washed with $300\text{ }\mu\text{L}$ of HISCL washing solution (Sysmex Corporation, #05423618) 3 times, $300\text{ }\mu\text{L}$ of PBS containing 1% BSA was added to each well of the plate, and the plate was incubated at room temperature for 1 h. The blocking buffer was removed from the wells, $100\text{ }\mu\text{L}$ of sample was transferred to the wells, and the plate was incubated at room temperature for 1 h with shaking at 600 rpm. After the wells were washed with $300\text{ }\mu\text{L}$ of HISCL washing solution 3 times, $100\text{ }\mu\text{L}$ of $0.1\text{ }\mu\text{g/mL}$ biotinylated anti-transferrin polyclonal antibody in PBS containing 1% BSA was added to the wells, and the plate was incubated at room temperature for 1 h with shaking at 600 rpm. The wells were washed 3 times, $100\text{ }\mu\text{L}$ of streptavidin-conjugated alkaline phosphatase (Vector Laboratories, Inc. #SA-5100) diluted with PBS containing 1% BSA was added to the wells 5000 times, and the plate was incubated at room temperature for 30 min. The wells were washed 6 times. Then, $100\text{ }\mu\text{L}$ of CDP-Star (Sysmex Corporation, #06,443,319) reagent was added to the wells, and the plate was incubated at room temperature for 15 min. Chemiluminescence was measured using a microplate reader. The ELISA results were standardized using TTR purified from human plasma as calibration samples.

Analytic validation of ELISA

Calibration curve analysis was performed by measuring calibration samples ($n = 3$). The standard curves of TTR were generated using a linear $1/\times$ regression of a calibrator. The precision was determined as the %CV of the analysis of each calibration sample. The accuracy was determined with the calibration standards as the back-calculated TTR concentrations. Dilution linearity was assessed by diluting pooled serum from 1/40,000 to 1/640,000, which covers the final dilution rate of serum used in the ELISA (1/61,800), in PBS containing 1% BSA before analysis and analyzed according to a previous study²⁶. Intra-assay precision (%CV) was determined by measuring the concentrations in 6 replicates of the control samples containing different concentrations (high: 8.3 ng/mL , medium: 4.8 ng/mL , low: 2.4 ng/mL) of recombinant wild-type TTR in a single ELISA assay. Inter-assay precision (%CV) was determined by analyzing the control samples in 6 different ELISA assays.

Assessment of TTR stability under urea conditions

The workflow for assessing TTR stability under urea conditions is shown in Fig. 1. Human serum, human serum preincubated with $500\text{ }\mu\text{mol/L}$ tafamidis (BOC Sciences, #B2693-463,292) at room temperature for 30 min, and $160\text{ }\mu\text{g/mL}$ recombinant TTRs in PBS containing 1% BSA were diluted tenfold with PBS containing 0 to 8 mol/L urea, resulting in a final concentration of 0– 7.2 mol/L urea, which was subsequently incubated at $25\text{ }^{\circ}\text{C}$ for 48 h. After incubation, the samples were diluted 6180 times with PBS containing 1% BSA. Tetrameric TTR levels in the samples were quantified using ELISA. TTR stability under urea conditions was evaluated as the residual TTR tetramer percentage and calculated using the following formula.

$\% \text{ Residual TTR tetramer ratio} = [\text{Tetrameric TTR levels in samples treated with each concentration of urea for 48 h at } 25\text{ }^{\circ}\text{C} / \text{Tetrameric TTR levels in samples treated with } 0\text{ mol/L urea for 48 h at } 25\text{ }^{\circ}\text{C}] \times 100.$

Gel filtration chromatography

An ÄKTA pure 25 system (Cytiva #29,014,831) with a Superdex 200 Increase 10/300 GL column (Cytiva #28-9909-44) was used to determine the molecular weight of recombinant TTR. The column was initially equilibrated with PBS. Subsequently, recombinant wild-type TTR and recombinant monomeric variant TTR (F87M/L110M) in PBS were loaded onto the column and eluted with the same buffer at a constant flow rate. The elution process was monitored by measuring absorbance at 280 nm. The molecular weights of these recombinant proteins were calculated by comparing their elution volumes with the calibration curve, which was generated using the elution volumes of an LMW calibration kit (Cytiva, #28-4038-41) and an HMW calibration kit (Cytiva, #28-4039-42).

Statistical analyses

Continuous variables are presented as means \pm standard deviations or medians with interquartile ranges depending on whether the data were normally or nonnormally distributed. Baseline characteristics were compared between controls and ATTRwt-CM patients. After the sample distribution was analyzed for normality using Kolmogorov–Smirnov tests, continuous variables were compared by using the unpaired Student's *t* test or the Mann–Whitney *U* test, as appropriate. Categorical variables were assessed by the χ^2 test. Differences between multiple groups were evaluated by one-way ANOVA, followed by Dunnett's post-test or by Kruskal–Wallis test, followed by Dunn's post-test after the sample distribution was tested for normality. A *P* value < 0.05 was considered to indicate statistical significance. All statistical analyses were carried out using Stata version 17.0 software (College Station) or GraphPad Prism software version 9.0 (GraphPad Software).

Data availability

Any data not included in this manuscript will be made available upon reasonable request to the corresponding author.

Received: 29 May 2024; Accepted: 28 August 2024

Published online: 03 September 2024

References

- Carroll, A. *et al.* Novel approaches to diagnosis and management of hereditary transthyretin amyloidosis. *J. Neurol. Neurosurg. Psychiatry* **93**, 668–678. <https://doi.org/10.1136/jnnp-2021-327909> (2022).
- Monaco, H. L., Rizzi, M. & Coda, A. Structure of a complex of two plasma proteins: Transthyretin and retinol-binding protein. *Science* **268**, 1039–1041. <https://doi.org/10.1126/science.7754382> (1995).
- Colon, W. & Kelly, J. W. Partial denaturation of transthyretin is sufficient for amyloid fibril formation in vitro. *Biochemistry* **31**, 8654–8660. <https://doi.org/10.1021/bi00151a036> (1992).
- Sun, X., Dyson, H. J. & Wright, P. E. Kinetic analysis of the multistep aggregation pathway of human transthyretin. *Proc. Natl. Acad. Sci. USA* **115**, E6201–E6208. <https://doi.org/10.1073/pnas.1807024115> (2018).
- Ruberg, F. L., Grogan, M., Hanna, M., Kelly, J. W. & Maurer, M. S. Transthyretin amyloid cardiomyopathy: JACC state-of-the-art review. *J. Am. Coll. Cardiol.* **73**, 2872–2891. <https://doi.org/10.1016/j.jacc.2019.04.003> (2019).
- Jiang, X. *et al.* An engineered transthyretin monomer that is nonamyloidogenic, unless it is partially denatured. *Biochemistry* **40**, 11442–11452. <https://doi.org/10.1021/bi011194d> (2001).
- Hammarstrom, P., Jiang, X., Hurshman, A. R., Powers, E. T. & Kelly, J. W. Sequence-dependent denaturation energetics: A major determinant in amyloid disease diversity. *Proc. Natl. Acad. Sci. USA* **99**(Suppl 4), 16427–16432. <https://doi.org/10.1073/pnas.202495199> (2002).
- Maurer, M. S. *et al.* Tafamidis treatment for patients with transthyretin amyloid cardiomyopathy. *N. Engl. J. Med.* **379**, 1007–1016. <https://doi.org/10.1056/NEJMoa1805689> (2018).
- Adams, D. *et al.* Patisiran, an RNAi therapeutic, for hereditary transthyretin amyloidosis. *N. Engl. J. Med.* **379**, 11–21. <https://doi.org/10.1056/NEJMoa1716153> (2018).
- Adams, D. *et al.* Efficacy and safety of vutrisiran for patients with hereditary transthyretin-mediated amyloidosis with polyneuropathy: A randomized clinical trial. *Amyloid* **30**, 1–9. <https://doi.org/10.1080/13506129.2022.2091985> (2023).
- Griffin, J. M. *et al.* ATTR amyloidosis: Current and emerging management strategies: JACC: CardioOncology state-of-the-art review. *JACC CardioOncol.* **3**, 488–505. <https://doi.org/10.1016/j.jacc.2021.06.006> (2021).
- Castano, A. *et al.* Unveiling transthyretin cardiac amyloidosis and its predictors among elderly patients with severe aortic stenosis undergoing transcatheter aortic valve replacement. *Eur. Heart J.* **38**, 2879–2887. <https://doi.org/10.1093/eurheartj/ehx350> (2017).
- Gonzalez-Lopez, E. *et al.* Wild-type transthyretin amyloidosis as a cause of heart failure with preserved ejection fraction. *Eur. Heart J.* **36**, 2585–2594. <https://doi.org/10.1093/eurheartj/ehv338> (2015).
- Lindmark, K., Pilebro, B., Sundstrom, T. & Lindqvist, P. Prevalence of wild type transthyretin cardiac amyloidosis in a heart failure clinic. *ESC Heart Fail.* **8**, 745–749. <https://doi.org/10.1002/ehf2.13110> (2021).
- Porcari, A. *et al.* Prevalence, characteristics and outcomes of older patients with hereditary versus wild-type transthyretin amyloid cardiomyopathy. *Eur. J. Heart Fail.* **25**, 515–524. <https://doi.org/10.1002/ehf.2776> (2023).
- Westin, O. *et al.* Screening for cardiac amyloidosis 5 to 15 years after surgery for bilateral carpal tunnel syndrome. *J. Am. Coll. Cardiol.* **80**, 967–977. <https://doi.org/10.1016/j.jacc.2022.06.026> (2022).
- Antonopoulos, A. S. *et al.* Prevalence and clinical outcomes of transthyretin amyloidosis: A systematic review and meta-analysis. *Eur. J. Heart Fail.* **24**, 1677–1696. <https://doi.org/10.1002/ehf.2589> (2022).
- Westermarck, P., Sletten, K., Johansson, B. & Cornwell, G. G. 3rd. Fibril in senile systemic amyloidosis is derived from normal transthyretin. *Proc. Natl. Acad. Sci. USA* **87**, 2843–2845. <https://doi.org/10.1073/pnas.87.7.2843> (1990).
- Ton, V. K., Mukherjee, M. & Judge, D. P. Transthyretin cardiac amyloidosis: pathogenesis, treatments, and emerging role in heart failure with preserved ejection fraction. *Clin. Med. Insights Cardiol.* **8**, 39–44. <https://doi.org/10.4137/CMC.S15719> (2014).
- Zhao, L., Buxbaum, J. N. & Reixach, N. Age-related oxidative modifications of transthyretin modulate its amyloidogenicity. *Biochemistry* **52**, 1913–1926. <https://doi.org/10.1021/bi301313b> (2013).
- Jiang, X. *et al.* A circulating, disease-specific, mechanism-linked biomarker for ATTR polyneuropathy diagnosis and response to therapy prediction. *Proc. Natl. Acad. Sci. USA* <https://doi.org/10.1073/pnas.2016072118> (2021).
- George, J. *et al.* A novel monoclonal antibody targeting aggregated transthyretin facilitates its removal and functional recovery in an experimental model. *Eur. Heart J.* **41**, 1260–1270. <https://doi.org/10.1093/eurheartj/ehz695> (2020).
- Rappley, I. *et al.* Quantification of transthyretin kinetic stability in human plasma using subunit exchange. *Biochemistry* **53**, 1993–2006. <https://doi.org/10.1021/bi500171j> (2014).
- Monteiro, C. *et al.* Predictive model of response to tafamidis in hereditary ATTR polyneuropathy. *JCI Insight* <https://doi.org/10.1172/jci.insight.126526> (2019).
- Connors, L. H. *et al.* Heart failure resulting from age-related cardiac amyloid disease associated with wild-type transthyretin: A prospective. *Observ. Cohort Stud. Circ.* **133**, 282–290. <https://doi.org/10.1161/CIRCULATIONAHA.115.018852> (2016).
- Iino, T. *et al.* Quantification of amyloid-beta in plasma by simple and highly sensitive immunoaffinity enrichment and LC-MS/MS assay. *J. Appl. Lab. Med.* **6**, 834–845. <https://doi.org/10.1093/jalm/jfaa225> (2021).

Author contributions

K.I.H., T.I., and R.T. designed and supervised the study. T.I. and M.N. wrote the manuscript. H.T., M.N., S.Y., and J.A. collected the serum of the patients. T.I., S.W., and A.H. performed the experiments. M.N. and M.S. analyzed the data. All authors reviewed the manuscript.

Funding

This work was supported by a Grant-in-Aid for Young Scientists (23K15102) from the Ministry of Education, Culture, Sports, Science and Technology of Japan and a Japan Heart Foundation Research Grant.

Competing interests

The authors declare no competing interests.

Additional information

Supplementary Information The online version contains supplementary material available at <https://doi.org/10.1038/s41598-024-71446-8>.

Correspondence and requests for materials should be addressed to M.N.

Reprints and permissions information is available at www.nature.com/reprints.

Publisher's note Springer Nature remains neutral with regard to jurisdictional claims in published maps and institutional affiliations.

Open Access This article is licensed under a Creative Commons Attribution-NonCommercial-NoDerivatives 4.0 International License, which permits any non-commercial use, sharing, distribution and reproduction in any medium or format, as long as you give appropriate credit to the original author(s) and the source, provide a link to the Creative Commons licence, and indicate if you modified the licensed material. You do not have permission under this licence to share adapted material derived from this article or parts of it. The images or other third party material in this article are included in the article's Creative Commons licence, unless indicated otherwise in a credit line to the material. If material is not included in the article's Creative Commons licence and your intended use is not permitted by statutory regulation or exceeds the permitted use, you will need to obtain permission directly from the copyright holder. To view a copy of this licence, visit <http://creativecommons.org/licenses/by-nc-nd/4.0/>.

© The Author(s) 2024